Analysis of The Effect Caused by Vibration Due to Fiber Bragg Grating Sensor Wavelength

Firda Wahyuningtyas[1], Amalia Eka Rakhmania[2*], Yoyok Heru Prasetyo Isnomo[3]

[1,3] Digital Telecommunication Network Study Program, Department of Electrical Engineering, State Polytechnic of Malang, 65141, Indonesia

[2] Telecommunication Engineering Study Program, Department of Electrical Engineering, State Polytechnic of Malang, 65141, Indonesia

[1]firdaawahyu23@gmail.com , [2]amaliaeka.rakhmania@gmail.com , [3]yoyok.heru@polinema.ac.id

***Abstract*— It is undeniable that fiber cables that are routed underground using the ducting method are susceptible to interference due to external factors such as vibration, especially if the soil is susceptible to vibration activity such as natural factors (earthquakes), heavy traffic, construction, or other human activities. The application of Fiber Bragg Grating sensors along fiber optic cable routes is one solution to facilitate maintenance and checking if data transmission problems occur. In this research, experimental research methods or system creation were used with the aim of the research being to have the final result in the form of an analysis of the influence of object vibrations on the output power and wavelength of the Fiber Bragg Grating Sensor. So, the data obtained in this research can be used as a reference for further research so that Fiber Bragg Grating can be used as a vibration sensor in underground cable routing for data telecommunications systems. The research results show that effective vibration measurements start from load variations of 4 grams to 10 grams and each load variation which is calculated as vibration results in a change in the FBG grating period so that the Bragg wavelength value will also change for each load. As a result of the vibration of the spring, there is a change in the average wavelength of delta lambda Bragg 1.5779 with a system RMS error of 1.19 which indicates the system is working well.**

Keywords*— *Bragg Grating Fiber, Bragg Wavelength, Data Transmission Interference, Optical Fiber, Spring Vibration.

I. INTRODUCTION

Currently, fiber optic cables are widely used by internet and telecommunications service providers to transmit images, voice messages and data. Communication using fiber optic cables is basically a data transmission technique from one location to another using light pulses [1].

In data transmission, the commonly used fiber optic cable routing methods are the duct method (cable routing from underground) and the aerial method (cable routing from the air) [2]. However, in Malang City, the aerial routing method is more widely applied compared to routing using the ducting method because it is considered more efficient, especially in terms of installation. However, as time goes by, cable installations using aerial methods are becoming increasingly massive and uncontrolled, even to the point of disturbing the comfort of the general public.

Quoted from Jawa Pos Radar Malang last February, fiber optic cables dangling on Jalan Kawi, Malang City, entangled two motorbike riders, causing traffic jams due to the cables running across them [3]. The case of irregular cable stranding in Malang City itself has received a warning from the Mayor of Malang since 2022 who threatened to cut cables to providers who do not pay attention to cable installation ethics and make the condition of electricity poles become irregular, precisely at the redlight intersection at the Sabilillah Mosque, District Blimbing [4].

As a result of these problems, the Malang City government has actively carried out outreach with internet and electricity service providers to switch cable routing methods to using the ducting method [5]. However, after reducing overhead cables and switching to using the ducting method, other problems arose that had to be faced by internet service providers, namely related to maintenance and handling troubleshooting which was not easy. When cables have been buried underground, it is undeniable that the cables are susceptible to interference due to external factors such as vibration, especially if the ground is susceptible to vibration activity such as natural factors (earthquakes), heavy traffic, construction, or other human activities [6].

For example, in the installation of fiber optic ducting cables in the Blimbing station area, where according to the SOP the cables are routed at a depth of 90 cm from the ground surface. At this depth, duct cables that have been wrapped in pipes that are routed for 300 meters across the tracks can still feel vibrations that occur at the ground surface, such as vibrations that occur when a train passes or vibrations during heavy traffic due to the vibration radius caused by a passing train. reach a distance of 2 meters from the train tracks [7]. However, the impact of train vibrations on the ground is usually not as strong as the impact of vibrations from an earthquake, and is often only felt as a mild vibration or shaking. However, this does not simply mean that vibrations

*Corresponding author

caused by vehicles are not harmful to the signal distribution of duct cables. Vibrations that occur continuously can also be dangerous and affect the bending of the cable and as a result will affect the wavelength of the transmitted signal or cause the server to go down [8]. Meanwhile, dealing with data transmission disturbances in ducting cables requires a short amount of time. Internet service customers must contact customer service from the internet provider used to carry out checks. After that, the technician on duty will carry out a field survey to determine the location and cause of interference with the cable for further treatment (data tracking at each data distribution point).

From the problems that have been presented, the application of Fiber Bragg Grating sensors along fiber optic cable routes is one solution to facilitate maintenance and checking if data transmission problems occur. In this research, data analysis was carried out to determine the effect of vibration on the wavelength of the Fiber Bragg Grating Sensor. So that the data obtained in this research can be used as a reference for further research so that Fiber Bragg Grating can be used as a vibration sensor for routing fiber optic cables in the ground.

Previous research developed a fiber optic temperature sensor system by utilizing changes in wavelength. So, apart from the problems previously stated, this research is also the basis for considering the research "Analysis of the Effect of Vibration on the Wavelength of the Fiber Bragg Grating Sensor" because the working principle of the FBG sensor is measuring the reflection of the Bragg wavelength by measuring the difference in the wavelength of the incoming light source. and the light that is reflected or passes through the sensor when vibration occurs [9] with the vibration concept will be obtained from the implementation of the spring oscillation concept which arises as a result of applying a tensile force to varying loads depending on the spring and results in a shift in wavelength to determine changes in the Bragg wavelength value.

Changes in wavelength due to spring vibrations will later be displayed on the Optical Spectrum Analyzer (OSA) in the form of a sine signal and the amount of output power released during the load throwing process can be determined from the Optical Spectrum Analyzer (OSA) and Optical Power Meter (OPM).

II. METHOD

In this study, experimental research methods or system construction were used with the aim of having the final result in the form of an analysis of the effect of object vibration on the wavelength and output power recorded in the form of a sine signal by the Optical Spectrum Analyzer. In this study, a sensor evaluation method was used where the main controller of the system was a hanging load which was subjected to a tensile force to trigger an oscillatory process on a spring attached to the coupler and recorded by the Fiber Bragg Grating Sensor for display on the Optical Spectrum Analyzer (OSA).

This research will later discuss the research design in the form of block design, system design and application, materials and tools used, and the determination of the spring vibration system procedure.

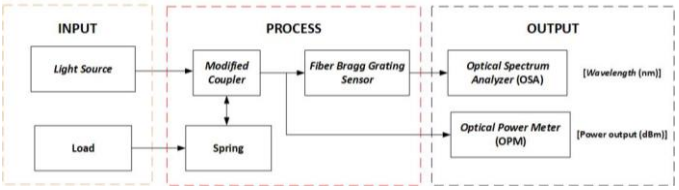

Figure 1. System block diagram

Based on shown in Figure 1, the system block diagram above, it can be explained Light Source as a light source that will be sent to the sensor. Fiber Bragg Grating (FBG) is a sensor that utilizes changes in the lattice spacing in it to reflect a certain wavelength. If the periodic lattice spacing changes, the Bragg wavelength (λ Bragg) will shift according to changes in the distance between the gratings on the FBG sensor. Spring as a tool that will vibrate seen from the deflection experienced by the spring when the load on the coupler is thrown. Load as an object that depends on a spring with a given weight variation to observe the change in wavelength and the output power generated because of the variation. Optical Spectrum Analyzer (OSA) used to measure and displays the distribution of power and wavelength of an optical source in a certain wavelength range. Optical Power Meter (OPM) used to measure the strength of the power in the optical signal so that the loss (loss) of light power on the fiber optic channel is known.

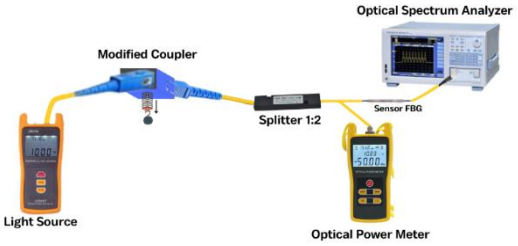

Figure 2. Mechanical design

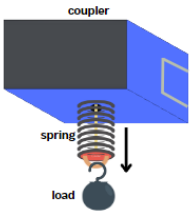

Figure 3. Coupler design (outside look)

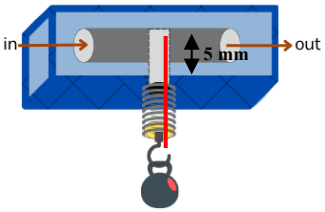

Figure 4. Coupler design (inside look)

Mechanical design as shown in Figure 2, is made to describe the mechanical design that will be implemented in research. The following is the mechanical design of the system along with the dimensions and descriptions that will be used in the study.

As shown in Figure 3 dan 4, the Fiber Bragg Grating sensor is placed on the fiber optic path, precisely at one of the 1:2 splitter outputs to the Optical Spectrum Analyzer. This is because when the load that depends on the spring is subjected to a 1 cm long tensile force, an oscillation or vibration process will occur in the spring which results in a shift in the reflection of the wavelength of light on the Fiber Bragg Grating sensor. The light source was obtained from a handheld light source with a wavelength of 1550 nm. The shift in wavelength when the load is ejected will be detected by a series of fiber optic sensors Fiber Bragg Grating and displayed on the Optical Spectrum Analyzer (OSA) in the form of a sine signal and on the Optical Power Meter (OPM) it will be known how much output power is released during the load ejection process.

After designing the system, the following will explain the research procedures carried out to obtain data are as follows:

1. Determine the load parameters used. In this study, 10 variations of the weight of the hanging load were used with a weight of 1 gram - 10 grams with an increase of 1 gram for each data collection.
2. Designing and connecting research tools in the form of light sources, SC-SC patch cords, modified couplers, springs, modified 1:2 splitters, Fiber Bragg Grating Sensors, OPM, and OSA.
3. Conducting tool testing by designing the system as a whole followed by initial testing that is adjusted to theoretical data
4. Conduct research when the initial test results are in accordance with theoretical data for further research by providing variations in experimental parameters.
5. The data collection process obtained from research is in the form of output power, wavelength values, and frequencies that appear on OPM and OSA.

The procedure below is the steps on how to change one of the SC Outputs on the Splitter to FC to be connected to Fiber Bragg Grating using an FC-FC adapter.

1. Prepare tools and materials in the form of a 1:2 splitter, FC-FC patch cord, cleaver, stripper pliers, sleeve protection, and fusion splicer
2. Cut one of the splitter outputs and the FC-FC patch cord
3. Strip each end of the cable (output splitter that has cut ends and pieces of FC patch cord) using stripper pliers and cut the core using a cleaver to get precise cut results
4. Insert the protection sleeve on the FC patch cord cable before connecting it with the splitter
5. Connect the output of the splitter cable that has been cut off with a piece of FC patch cord using a fusion splicer
6. Position the protection sleeve right at the core connection and heat it using the heater feature on the fusion splicer to glue the protection sleeve with the core connection so that the connection is not easily broken

The procedure below is the steps how measuring fiber optic network power and wavelength using an Optical Spectrum Analyzer (OSA)

1. Turn on OSA by pressing the power button and wait for the initializing process to finish as shown in Figure 5 below

Figure 5. Display OSA When Ready to Use

2. Connect the fiber optic circuit output you want to measure with the OSA optical input port, as shown in Figure 6 below

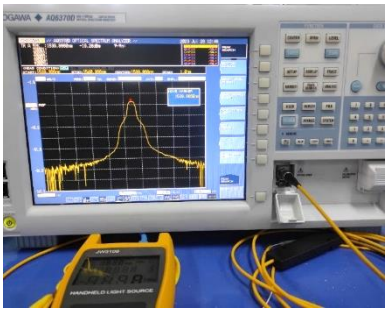

Figure 6. OSA Connected to a Light Source

3. Press the program button > select an available program > execute program. OSA will automatically load and display wave results on the screen
4. The SWEEP button contains functions related to sweeping or data switching. When you press the SWEEP button, the soft key menu for sweeping appears. In this measurement, the Single soft key is used to retrieve spring data in a stationary condition and select the Auto soft key to capture real-time moving data
5. The SPAN button contains functions related to setting the measured wavelength range or frequency range. The soft key function changes according to whether the screen display mode is wavelength display mode or frequency display mode
6. The MARKER button contains functions related to markers to see wave conditions at a certain point
7. The PEAK SEARCH button contains functions for automatic searching for peaks and bottoms in a measured waveform.
8. To find out the power value measured in the waveform, you can use the peak search button, then the display at the top center will appear how much power is measured in the signal wave.

There are several reasons why the signal peak was chosen:

a. Main Signal Detection: the signal peak helps in

identifying and separating the main signal from noisy or interference signals. In communications, for example, when receiving a transmitted signal, it is important to isolate the main signal from weaker signals or interference.

b. Sensitivity and Accuracy: The peak of a signal is usually the highest point in the signal, which means it is the strongest part and is easier to identify numerically. Measuring the peak of the signal can provide results that are quite sensitive and accurate in detecting the presence and characteristics of the signal.
c. Power or Amplitude Measurement: The signal peak is the place where the power or amplitude reaches its maximum. For example, in spectrum analysis, knowing where the signal peaks are can provide information about the dominant frequency in that signal.
d. Modulation and Demodulation: In wireless communication, signal modulation and demodulation are often involved. Signal peak selection can assist in the demodulation process by identifying where the modulation signal passes through its peak in the waveform.
e. Signal Processing Algorithms: Many signal processing algorithms are designed to work with signal peaks. For example, in a peak detection algorithm, the goal is to identify peak points in a signal.

III. RESULT AND DISCUSSION

Figure 7. Overall System Network

A. *Initial Circuit Measurement Results*

In Figure 7 is shown overall system network, and Table I presents the detailed loss measurements for each network component used in the system. The table compares the standard loss values with the measured loss results for components such as patch cords, splitters, couplers, connectors, and fiber Bragg grating, highlighting the attenuation contributed by each element. These measurement results provide an initial assessment of network performance and serve as a reference for evaluating overall system losses.

TABLE I
LOSSES IN NETWORKS

No.	Description	Loss Standard (dB) [27]	Total	Loss Measurement Result (dB)
1.	Patch cord SC-SC	0.25	1	1.46
2.	Splitter 1:2	3.70	1	6.58
3.	Coupler Adapter	0.1		
4.	Modified Coupler		1	13.04
5.	Connection pada output 2 splitters	0.1	1	0.03
6.	Connection pada input splitter	0.1	1	0.05
7.	Iron connector FC-FC	0.1	1	0.1
8.	Fiber Bragg Grating	3	1	5.87

B. *System Test Results*

1) Measurement Results of the Effect of Load Variations Assumed as Vibration on Output Power and System Wavelength

In this sub-chapter, measurements are made of the output power parameters and wavelength which are influenced by applying a pulling force to a load 1 cm long from the equilibrium position for each load hanging on the spring, resulting in an oscillation or vibration process in the spring. From the results of measuring changes in spring length with varying loads, the value of the spring constant (k) is obtained which can be calculated using equation below where $k = \frac{m.g}{x}$ with g = 9.807 m/s^2 which is shown in Table 2. The following is an example of a calculation for an 8-gram load, as shown at Equation (1) and (2).

$$k = \frac{m.g}{x} \quad (1)$$

$$k = \frac{0{,}008 \times 9.807}{0.004} = 19.614\ N/m \quad (2)$$

For constant values for other load variations, see the Table II below.

TABLE II
SPRING CONSTANT VALUES FOR EACH LOAD

Load (kg)	x_0 (cm)	x_1 (cm)	$x = x_1 - x_0$ (m)	k (N/m)
0	3.2	3.2	0	error
0.001	3.2	3.2	0	error
0.002	3.2	3.25	0.0005	39.228
0.003	3.2	3.3	0.001	29.421
0.004	3.2	3.35	0.0015	26.152
0.005	3.2	3.4	0.002	24.518
0.006	3.2	3.45	0.0025	23.537
0.007	3.2	3.5	0.003	22.883
0.008	3.2	3.6	0.004	19.614
0.009	3.2	3.65	0.0045	19.614
0.01	3.2	3.7	0.005	19.614
Average Spring Constant (from 4 – 10 gram)				22.276

Because the spring constant value is not constant due to changes in the length of the spring during loading, the direct measurement results are not the same as in theory, for the next calculation the average value of the spring constant is used, namely k = 22,276 N/m taken from a load range of 4 grams to 10 grams. grams because in the load range of 0 grams to 3 grams the system is still in a loss condition. Once the spring constant value is known, using equation below, the value of the oscillation frequency (Hz) can be determined to determine

the number of vibrations that occur in 1 second for each load variation imposed on the spring, as shown at Equation (3) below:

$$f = \frac{1}{2\pi}\sqrt{\frac{k}{m}}, \pi = 3{,}14, k = 22.276\ N/m \quad (3)$$

For example, at a load of 4 grams, the oscillation frequency experienced by the system, as shown at Equation (4) below:

$$f = \frac{1}{2 \times 3{,}14}\sqrt{\frac{22.276}{0.004}} = 17.16\ \text{Hz} \quad (4)$$

The oscillation frequency values for each load in more detail are shown in Table III below.

TABLE III
OSCILLATION VIBRATION VALUES IN SPRINGS FOR EACH LOAD

Beban (gram)	f (Hz)
0	error
1	error
2	219.88
3	155.48
4	117.16
5	104.79
6	95.66
7	88.57
8	82.85
9	78.11
10	74.10

From Table 3 it is found that the greater the weight of the load imposed on the spring, the smaller the resulting frequency will be due to changes in the spring amplitude point.

2) Effect of Load Weight Variations on Spring Vibration

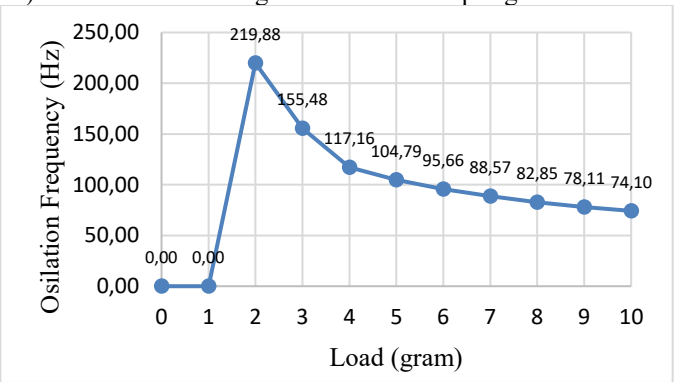

Figure 8. The Effect of Varying Load Weight on Spring Vibration Graph

The load hanging on the spring is subjected to a tensile force of 1 cm to trigger spring oscillation. Figure 8 shows the value of the oscillation frequency or vibration experienced by the spring within 1 second for each load variation obtained from the results of theoretical calculations because the graph shows that the value of the spring vibration or oscillation frequency produced in the system is very high. Meanwhile, the spring amplitude (maximum rate of movement of the load from the balance position) is very small. If the frequency value is very high, but the amplitude is very small, the movement of the object may not be visible easily to the human eye because the displacement is very small in a short time. In Figure 8, it is known that there is no vibration when the load is 0 gram and 1 gram because at this weight there is no change in the length of the spring.

However, the presence of a value in the spring frequency for a load weight of 2 grams to 10 grams indicates that the spring experiences vibrations regardless of the value. And the presence of vibrations indicates that a spring oscillation process has occurred which in this study resulted in a change in the position of the barrier which affected the test parameters, namely the output power and the wavelength of the transmitted light.

3) Effect of Load Variations on Output Power and Circuit Power Loss (System without FBG)

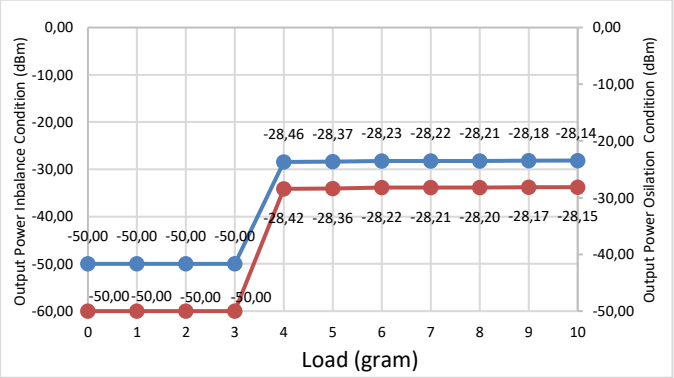

Figure 9. Effect of Load Variations on Circuit Output Power Without FBG on OPM Graph

The output power value taken during unbalance conditions and during oscillation in Figure 9 is the average value of three power measurement processes on the OPM for each condition. The output power value in unbalance conditions is obtained when the load hanging on the spring is at rest. Meanwhile, during the oscillation process, the output power value is obtained when the load is given a pull of 1 cm to trigger the oscillation process and reaches the spring amplitude point (the spring's maximum displacement point from the balance position).

From Figure 9 it is known that the OPM reaches a maximum value of -50.00 dBm in the load range of 0 to 3 grams, which means that the light source cannot be transmitted even though there has been a decrease in the barrier due to the load reaching 1 mm. In the two pictures above, it can be seen that there is a significant change in the output power when the spring is given a load of 4 grams, which indicates that the light source can only be distributed when the barrier has dropped to 1.5 mm, starting from a load weight of 4 grams to a load weight of 10 grams, which indicates that There are no obstructions in the transmission line at the coupler.

The data in the figure can be interpreted to mean that the position of the barrier on the coupler during unbalance conditions is higher than during oscillation. Thus, the output power value during the oscillation process is higher than the

output power value in unbalance conditions. A higher power value indicates that the power loss experienced during the transmission process is smaller as can be seen in Figure 10 below.

Based on these observations, the variation in output power clearly reflects the mechanical influence of the load on the optical transmission characteristics of the system. As the load increases, the displacement of the spring causes a corresponding change in the coupler barrier position, which directly affects the level of attenuation experienced by the transmitted light. This behavior demonstrates that the system is sensitive to small mechanical displacements, and the measured output power can be used as a reliable indicator of changes in loss due to both static (unbalance) and dynamic (oscillation) conditions.

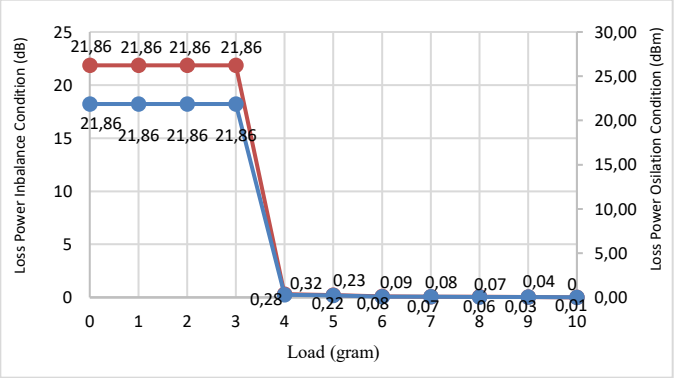

Figure 10. Effect of Load Variations on Circuit Power Loss Without FBG on OPM Graph

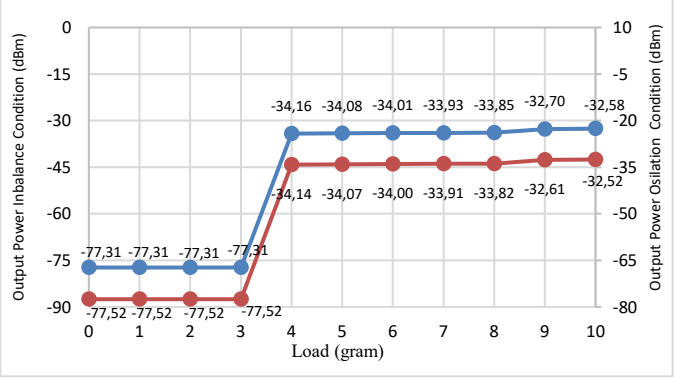

Figure 11. Effect of Load Variations on Circuit Output Power Without FBG on OSA Graph

The output power values taken during unbalance and oscillation conditions in Figure 11 are the average values from three power measurement processes at the OSA for each condition. From Figure 11, it is known that the signal transmission process is said to be a loss if the output power recorded on the OSA has reached a value of -77 dBm or below, which applies in the load range of 0 to 3 grams, which means that the light source in that range cannot be transmitted.

In OSA, it was also measured that the output power value during the oscillation process was higher than the output power value in unbalance conditions with the range of output power values in OSA being more significant compared to measurements using OPM. The heavier the load hanging on the spring, the greater the output power value received and this indicates that the power loss experienced during the transmission process is smaller as can be seen in Figure 12 below.

These results further confirm that the mechanical loading of the spring plays a crucial role in determining the optical transmission performance of the system. As the applied load increases, the resulting spring displacement improves the coupling condition by reducing the obstruction at the coupler, leading to higher output power levels observed on the OSA. This trend indicates that the system exhibits a clear correlation between mechanical displacement and optical loss behavior, demonstrating its capability to reliably capture transmission changes under both unbalance and oscillation conditions.

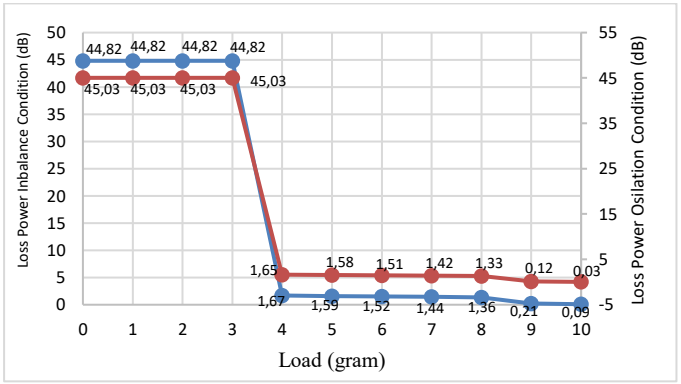

Figure 12. Effect of Load Variations on Circuit Power Loss Without FBG on OSA Graph

4) Effect of Load Variations on Output Power and Circuit Power Loss (System with FBG)

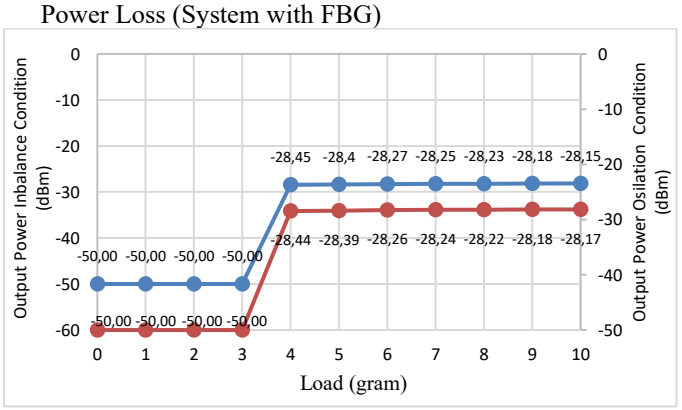

Figure 13. Effect of Load Variations on Circuit Output Power Using FBG on OPM Graph

The output power value taken during unbalance and oscillation conditions in Figure 13 is the average value of three power measurement processes on the OPM for each condition. The output power value in unbalance conditions is obtained when the load hanging on the spring is at rest.

Meanwhile, during the oscillation process, the output power value is obtained when the load is given a pull of 1 cm to trigger the oscillation process and reaches the spring amplitude point (the spring's maximum displacement point from the balance position).

From Figure 13 it is known that the OPM reaches a maximum value of -50.00 dBm in the load range of 0 to 3 grams, which means that the light source cannot be transmitted even though there has been a decrease in the barrier due to the load reaching 1 mm. In the two pictures above, it can be seen that there is a significant change in the output power when the spring is given a load of 4 grams, which indicates that the light source can only be distributed when the barrier has dropped to 1.5 mm, starting from a load weight of 4 grams to a load weight of 10 grams, which indicates that There are no obstructions in the transmission line at the coupler.

At a weight of 9 grams, the output power value at the unbalance position and during oscillation is the same. This can happen because the power values displayed in the tables and graphs are the average values from three measurement processes, where in measurements 2 and 3 the output power value when oscillations were recorded was not higher than when the load was in unbalance. Likewise, for a 10-gram load, the output power value during oscillation is even lower than during unbalance conditions. This is because at a load of 10 grams the condition of the transmission line on the coupler is no longer obstructed. So, even though during oscillation the position of the barrier is lower than during unbalance conditions, this does not affect the output power value much.

In Figure 14 below, it can be seen that providing load variations has an effect on the circuit power loss value. The greater the weight of the load hanging on the spring, the smaller the value of power loss produced during the data transmission process.

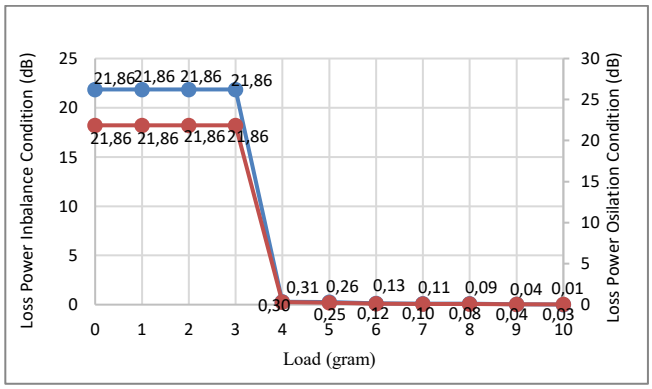

Figure 14. Effect of Load Variations on Circuit Power Loss Using FBG on OPM Graph

The output power value taken during unbalance and oscillation conditions in Figure 15 is the average value of three power measurement processes at the OSA for each condition. From Figure 15 it is known that the signal transmission process is said to be a loss if the output power recorded on the OSA has reached a value of -77 dBm or below for unbalance conditions and -73 or below during the oscillation process. Where this applies to the load range of 0 to 3 grams, which means that the light source in that range cannot be distributed.

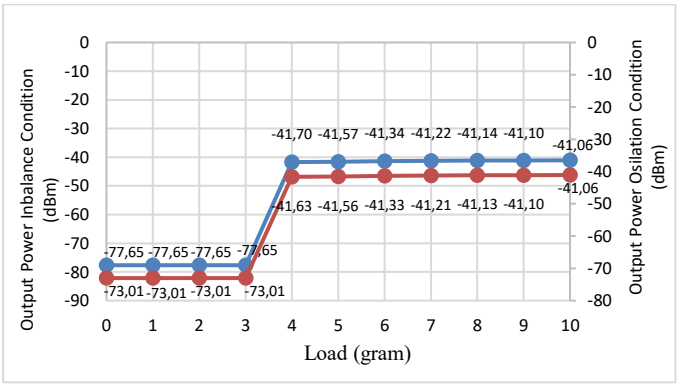

Figure 15. Effect of Load Variations on Circuit Output Power Using FBG on OSA Graph

In Figure 15, the output power value in the load range of 4 grams to 10 grams is around -41 dBm, where there has been a fairly large change from the results of measuring the power value of the circuit without Fiber Bragg Grating in the OSA. This happens because Fiber Bragg Grating itself has power loss like patch cords in general. So, the increase in the output power value after the FBG circuit is installed is not a bad thing because the power loss generated during the data transmission process is not large as can be seen in Figure 16 below.

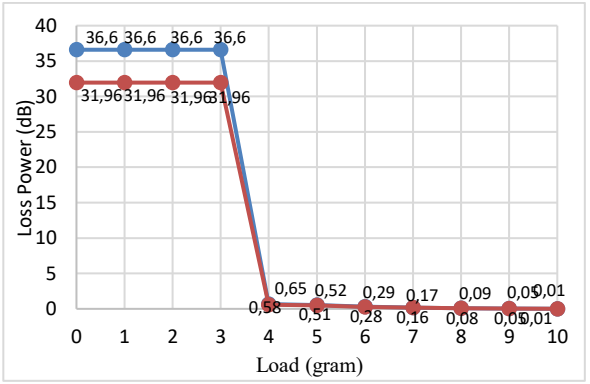

Figure 16. Effect of Load Variations on Circuit Power Loss Using FBG on OSA Graph ((-) Unbalance Condition, (-) Oscillation Condition)

5) Effect of Load Variations Calculated as Vibrations in the Spring on the Wavelength of the Fiber Bragg Grating Sensor

Figure 17 shows that during the spring oscillation process there is a change in the wavelength range received from the circuit using the FBG and the circuit without using the FBG. Before using Fiber Bragg Grating (FBG), the effective wavelength range received was between 1538.4440 nm to 1538.3240 nm referring to the conditions where light signals could begin to be transmitted, namely at a load of 4 grams to 10 grams. After using FBG, the effective wavelength range received is from 1539.9480 nm to 1539.9841 nm.

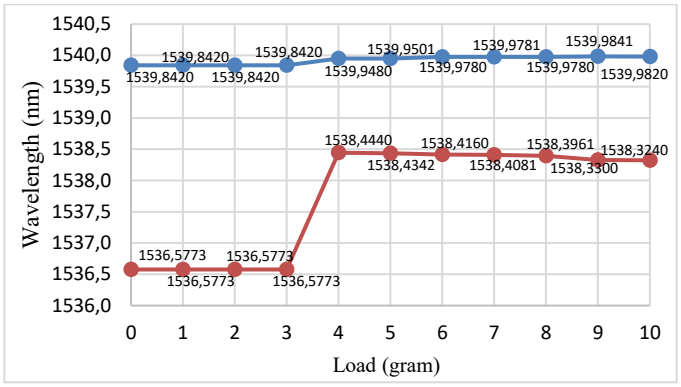

Figure 17. Comparison of the Effect of Load Variations on Wavelength during Oscillation (Maximum Spring Stretch) Graph ((-) With FBG, (-) Without FBG)

From the measurement results, the lambda shift value (Δλ) can be determined as shown at Equation (5)

$$\Delta\lambda_{Bragg} = \lambda\text{end} - \lambda\text{start} \quad (5)$$

Using above equation it is known that $\Delta\lambda_{0-3gr}$ = 3.2647 nm, $\Delta\lambda_{4gr}$ = 1.5040 nm, $\Delta\lambda_{5gr}$ = 1.5159 nm, $\Delta\lambda_{6gr}$ = 1.5620 nm, $\Delta\lambda_{7gr}$ = 1.5700 nm, $\Delta\lambda_{8gr}$ = 1.5819 nm, $\Delta\lambda_{9gr}$ = 1.6541 nm, dan $\Delta\lambda_{10gr}$ = 1.6580 nm. So on the average value of $\Delta\lambda_{Bragg}$ from the weight range of 4 gram to 10 gram = 1.5779 nm.

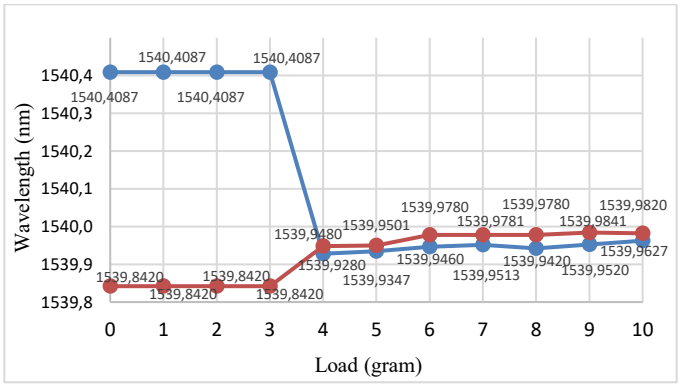

Figure 18. Effect of Load Variations on the Wavelength of a Circuit Using a Fiber Bragg Grating Sensor Graph ((-) Unbalance Condition, (-) Oscillation Condition)

Figure 18 shows that the vibrations that arise as a result of applying a tensile force of 1 cm to load variations have an effect on changes in the effective wavelength recorded by the OSA. The change in wavelength indicates that there has been a change in the grating period (Λ) due to vibrations which results in the reflection of certain wavelengths by the FBG. The wavelength reflected by the FBG is called the Bragg wavelength (λ_{Bragg}). To find out more about the value of λ_{Bragg}, look at Figure 19 below.

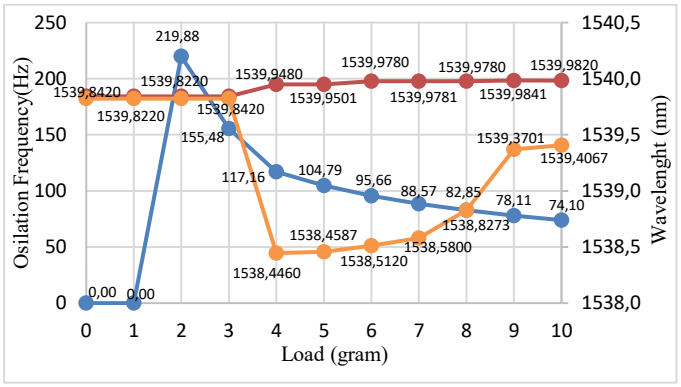

Figure 19. Comparison of the Effect of Load Variations Calculated as Vibrations on the FBG Wavelength in the Circuit Graph ((-) Spring Vibration, (-) Maximum Strain Wavelength, (-) Minimum Strain Wavelength)

Figure 19 shows the relationship between the frequency of the spring and the wavelength value obtained as a result of varying the load depending on the spring which is subjected to a 1 cm long pull to trigger oscillations so that vibrations appear in the spring which is one of the factors causing the change in wavelength.

From the measurement results, it was found that the wavelength range for each load variation was calculated as vibration from maximum to minimum spring position. From this range, it will be known what value of wavelength is reflected by the FBG Sensor (λ_{Bragg}) during the oscillation process because the wavelength that is not transmitted (the wavelength absorbed by the FBG) can be considered as the reflected wavelength and the value of this wavelength shorter than the original wavelength transmitted through the FBG.

The value of λ_{Bragg} can be found using the following Equation (6):

$$\lambda_{Bragg}\ (\text{nm}) = \text{Minimum Wavelength Range} - 0.01 \quad (6)$$

Where 0.01 is the minimum value of the λ_{Bragg} shift. The following is an example of a calculation to find the λ_{Bragg} value at a load of 0 grams.

$$\Lambda_{Bragg} = 1539.8220 - 0.01 = 1539.8120 \text{ nm}$$

The λ_Bragg value for other load variations will be shown further in Table IV below.

TABLE IV
BRAGG WAVELENGTH VALUES DUE TO LOAD VARIATIONS CALCULATED AS VIBRATIONS

Load (gr)	Oscillation Frequency (Hz)	Wavelength Range (nm)	λ_{Bragg} (nm)
0	error	1539.8220 – 1539.8420	1539.8120
1	error	1539.8220 – 1539.8420	1539.8120
2	219.88	1539.8220 – 1539.8420	1539.8120
3	155.48	1539.8220 – 1539.8420	1539.8120
4	117.16	1538.4460 – 1539.9480	1538.4360
5	104.79	1538.4587 – 1539.9501	1538.4487
6	95.66	1538.5120 – 1539.9780	1538.5020
7	88.57	1538.5800 – 1539.9781	1538.5700
8	82.85	1538.8273 – 1539.9780	1538.8173
9	78.11	1539.3701 – 1539.9841	1539.3601
10	74.10	1539.4067 – 1539.9820	1539.3967

If the value of λ_{Bragg} is known at Equation (7) and (8), then the value of the lattice period (Λ) of the FBG due to vibration can also be known with value of n_{eff}= 1.43

$$\Lambda_{Bragg} = 2 \, . \, n_{eff} \, . \, \Lambda \quad (7)$$

$$\Lambda = \frac{\lambda_{Bragg}}{2 \, . n_{eff}} \quad (8)$$

The following is an example of a calculation to find the Λ value for a 4-gram load.

$$\Lambda = \frac{1538.4360}{2 \, . 1,43} = 537.9147 \text{ nm}$$

The value of the grid period (Λ) for other load variations will be shown further in Table V below.

TABLE V
GRATING PERIOD VALUES DUE TO LOAD VARIATIONS CALCULATED AS VIBRATIONS

Load (gram)	Oscillation Frequency (Hz)	λ_{Bragg} (nm)	Λ (nm)
0	error	1539.8120	538.3958
1	error	1539.8120	538.3958
2	219.88	1539.8120	538.3958
3	155.48	1539.8120	538.3958
4	117.16	1538.4360	537.9147
5	104.79	1538.4487	537.9191
6	95.66	1538.5020	537.9378
7	88.57	1538.5700	537.9615
8	82.85	1538.8173	538.0480
9	78.11	1539.3601	538.2378
10	74.10	1539.3967	538.2506

$$\Delta\lambda_{Bragg} = \lambda_B \, (1 - p_e \,) \, \varepsilon \quad (9)$$

while p_e = 0,22 and ε = x (Table III)
Example of calculating $\Delta\lambda_{Bragg}$ using Equation (9) at a load of 4 grams:

$$\Delta\lambda_{Bragg} = \lambda_B \, (1 - p_e \,) \, \varepsilon$$
$$= 15388{,}4360 \, (1 - 0{,}22) \, 0{,}0015$$
$$= 1{,}8$$

Complete value data will be shown in Table VI below.

TABLE VI
$\Delta\Lambda_{BRAGG}$ VALUE FROM CALCULATION RESULTS

Load (gram)	$\Delta\lambda_{Bragg}$ (nm)
0	-
1	-
2	0.6005
3	1.2011
4	1.8000
5	2.4000
6	3.0001
7	3.6003
8	4.8011
9	5.4032
10	6.0036

Because in the condition of 0 to 3 grams the circuit is in a state of loss, the calculation of the RMS Error value only uses a load variation range of 4 grams to 10 grams. The RMSE equation can be seen in Equation (11) below.

$$\text{RMSE} = \sqrt{\frac{1}{n}\sum_i^n (y_i - \hat{y}_i)^2} \quad (10)$$

Description:
n = number of observations
y_i = actual observed value for the ith observation
$\hat{y}_i$ = value predicted by the model for the i-th observation

$$\text{RMSE} = \sqrt{\frac{1}{7}(0.5440 + 0.9403 + 1.1992 + 1.4249 + 1.7942 + 1.9362 + 2.0846)}$$

$$\text{RMSE} = \sqrt{\frac{1}{7}(9.9234)}$$

$$\text{RMSE} = \sqrt{1.4176}$$

$$\text{RMSE} = 1.19$$

From a series of measurement results, it was found that vibrations in the spring resulted in changes in the lattice period of the Fiber Bragg Grating Sensor where changes in the lattice period in the FBG showed that the FBG functioned as a selective reflector at certain wavelengths, while other wavelengths would be transmitted without much influence and recorded on the OSA.

Thus, the change in wavelength received during the spring oscillation process shows that the FBG has succeeded in directing light in a certain wavelength range, which can be used as a theoretical basis for further research that the Fiber Bragg Grating Sensor can be used in various applications, such as FBG can used to monitor vibrations in underground fiber optic cable routes to assist providers in monitoring data transmission conditions along cable routes.

IV. CONCLUSION

Based on the results of this research, it can be concluded that variations in load weight are directly proportional to the output power and inversely proportional to the power loss, meaning that heavier loads result in higher received output power and lower power loss during the light transmission process. Load variations that are manifested as vibrations also cause changes in the Fiber Bragg Grating wavelength ($\Delta\lambda_{Bragg}$), as each change in load alters the grating period, leading to a corresponding shift in the Bragg wavelength; larger load variations produce greater wavelength shifts with an average $\Delta\lambda_{Bragg}$ of 1.5779 nm. Furthermore, the Fiber Bragg Grating sensor demonstrated high performance, achieving an accuracy of 99.48% in wavelength measurement under vibration influence, with a system RMS error of 1.19, indicating that the overall system operates effectively and reliably.

REFERENCES

[1] H. Jusuf, "Perencanaan Jaringan Komunikasi Serat Optik Di Pulau Madura Untuk Mendukung Pembelajaran Jarak Jauh," pp. 8-9, 2021.

[2] L. M. Silalahi and F. A. Silaban, "Implementasi Jaringan Fiber To The Building Menggunakan Teknologi di Gedung Pasaraya Blok M," *JREC (Journal of Electrical and Electronics),* vol. 8, no. 2, pp. 91-100, 2020.

[3] Y. S. W. Wicaksana, "Kabel Menjuntai di Jalan Kawi Jerat Dua Pemotor," Jawa Pos Radar Malang, Kota Malang, 2023.

[4] N. Perdana and Krisiandi, "Kabel Semrawut di Kota Malang, Wali Kota Ancam Potong Milik Provider Nakal," Kompas.com, Malang dan Batu, 2022.

[5] M. Sampurno, "Rencana Penanaman Kabel di Kajoetangan, hanya PLN Belum Beri Kepastian," Jawa Pos Radar Malang, Kota Malang, 2022.

[6] Kartiria, Erhaneli and A. Y. Yudistia, "Analisis Penyebab Gangguan Jaringan Akses FFTH Untuk Layanan Internet pada PT. Telkom Indonesia Wilayah Pariaman," *JTE-ITP (Jurnal Teknik Elektro Institut Teknologi Padang),* vol. 11, no. 1, pp. 16-21, 2022.

[7] D. Khan and R. Burdzik, "Measurement and Analysis of Transport Noise and Vibration: A Review of Techniques, Case Studies, and Future Directions," *Measurement,* p. 113354, 2023.

[8] R. F. Sembiring, "Analisa Pengaruh Lekukan Bertekanan Pada Serat Optik Single Mode Terhadap Pelemahan Intensitas Cahay," *Jurnal Penelitian Rumpun Ilmu Teknik,* vol. 1, no. 2, pp. 01-05, 2022.

[9] F. N. Hidayah and H. Haikal, "ANALISIS PEMBEBANAN TERHADAP PANJANG GELOMBANG CAHAYA BERBASIS SENSOR FIBER BRAGG GRATING (FBG)," *Teknika,* vol. 3, no. 3, pp. 116-122, 2022.

[10] Y. H. P. Isnomo, M. N. Zakaria, M. Junus, M. A. Anshori and A. Aisah, "Optical Fiber Temperature Sensor Design," *In IOP Conference Series: Materials Science and Engineering ,* vol. 732, no. 1, p. 012108, 2020.

[11] Z. He, Z. Zhang , L. Li, Y. Zhan, W. Mi and Y. Feng , "A novel fiber Bragg grating vibration sensor with double equal-strength cantilever beams," *Optoelectronics letters,* vol. 17, no. 6, pp. 321-327, 2021.

[12] T. Li, J. Guo, Y. Tan and Z. Zhou, "Recent advances and tendency in fiber Bragg grating-based vibration sensor: A review," *IEEE Sensors Journal,* vol. 20, no. 20, pp. 12074-12087, 2020.

[13] L. Wei, D. Jiang , L. Yu, H. Li and Z. Liu, "A Novel Miniaturized FBG Vibration Sensor," *IEEE Sensors Journal,* vol. 19, no. 24, pp. 11932-11940, 2019.

[14] "SMK Negeri 5 Batam," 7 April 2022. [Online]. Available: https://smkn5batam.sch.id/2022/04/07/fiber-optik/. [Accessed 8 December 2022].

[15] H. Xu, F. Li, Y. Gao and W. Wang, "Simultaneous measurement of tilt and acceleration based on FBG sensor," *IEEE Sensors Journal,* vol. 20, no. 24, pp. 14857-14864, 2020.

[16] B. Yilmaz and A. Dolma, "Analysis of the Effect of Loss and Dispersion on Light Pulse in Fiber Optic Networks," *IEEE,* pp. 1-4, 2022.

[17] S. J. R. Guzman, C. R. Guzman and G. A. A. Castillo, "Optical sensing using fiber-optic multimode interference devices," *nonconventional sensing schemes,* vol. 21, no. 5, p. 1862, 2021.

[18] H. A. Haudungan, A. H. Rambe and L. A. Siregar, "Analisis Karakteristik Kabel Serat Optik Sebagai Media Transmisi Data," *In Prosiding Seminar Nasional Sosial, Humaniora, dan Teknologi,* pp. 22-31, 2022.

[19] D. Rahman, "Telkom University," 2 May 2023. [Online]. Available: https://bte-jkt.telkomuniversity.ac.id/2023/05/02/spektrum-elektromagnetik/. [Accessed 11 September 2023].

[20] "idschool," [Online]. Available: https://idschool.net/smp/rumus-periode-dan-frekuensi-pegas/. [Accessed 8 November 2022].

[21] R. Fauziyyah, "Telkom University," Kompas.com, 2020.

[22] T. M. I. Lab., "FBG Fiber-optic Sensing System," Tokyo Measuring Instrument Lab., Tokyp.

[23] Nasrulloh, A. Syahriar and R. N. Prasetyono, "Pengaruh Sensitivitas Suhu dengan Mode Couple-Mode terhadap Fiber Bragg Grating Fiber Optik," *avitec,* vol. 3, no. 2, pp. 139-148, 2021.

[24] Z. Xie, Y. Tan, B. Huang, D. Jiang and H. Liu, "High sensitivity fiber Bragg grating acceleration sensor based on rigid hinge," *IEEE Sensors Journal,* vol. 20, no. 15, pp. 8223-8231, 2019.

[25] H. Khlaifi, A. Zrelli and T. Ezzedine, "Optical fiber sensors in border detection application: Temperature, strain and pressure distinguished detection using fiber Bragg grating and fluorescence intensity ratio," *Optik,* vol. 229, pp. 166-257, 2021.

[26] "NextFiber," 2015. [Online]. Available: http://nextfiber.id/#elementor-action%3Aaction%3Dpopup%3Aopen%26settings%3DeyJpZCI6IjQ2NjYiLCJ0b2dnbGUiOmZhbHNlfQ%3D%3D. [Accessed 7 November 2022].

[27] Firdaus, F. A. Pradana and E. Indarto, "PERFORMANSI JARINGAN FIBER OPTIK DARI SENTRAL OFFICE HINGGA KE PELANGGAN DI YOGYAKARTA," *Jurnal Elektro Telekomunikasi Terapan,* vol. 3, no. 1, pp. 207-214, 2016.